物 理 化 学 学 报

Acta Phys. -Chim. Sin. **2020,** *36* (1), 1904066 (1 of 7)

[Article] doi: 10.3866/PKU.WHXB201904066 www.whxb.pku.edu.cn

Swelling Characteristics of g-C_3N_4 as Base Catalyst in Liquid-Phase Reaction

Jiequn Wu, Weiming Hua, Yinghong Yue *, Zi Gao

Department of Chemistry and Shanghai Key Laboratory of Molecular Catalysis and Innovative Materials, Fudan University, Shanghai 200438, P. R. China.

Abstract: Graphitic carbon nitrides (g-C_3N_4) with different surface areas were prepared by pyrolysis using different precursors including melamine, dicyandiamide, thiourea and urea, and subsequently characterized by X-ray diffraction (XRD), scanning electron microscopy (SEM), Fourier transform infrared spectra (FTIR), X-ray photoelectron spectroscopy (XPS), thermal gravimetric analysis (TGA) and N2 adsorption. Their basicities were measured by temperature-programmed desorption of CO_2 (CO_2-TPD) and acid-base titration. The catalytic properties for the Knoevenagel condensation of benzaldehyde and malononitrile were investigated in various solvents. In non-polar toluene solution, the benzaldehyde conversions of the g-C_3N_4 catalysts were low and changed according to their respective surface areas and basicities. However, in polar ethanol solution, the benzaldehyde conversions of all catalysts were similar, and much higher than those in toluene. This could not be explained by the results obtained from either of the two conventional basicity measurements. Further experimental results proved that g-C_3N_4 catalysts swelled in polar solutions, and more basic sites were exposed on the surface of the swollen catalysts, leading to the imminent increase in catalytic activity. This was proved by the catalyst poisoning data, which showed that the g-C_3N_4 catalyst lost its activity completely in toluene by adding 40.9 mmol·g^{-1} benzoic acid, while the same catalyst was still active in ethanol until the added amount exceeded 143.3 m·g^{-1}. Additionally, the reaction tests in various solutions showed that the swelling effect was enhanced according to the polarity of the solvent used. A similar conclusion could be reached for the Knoevenagel condensation of furfural and malononitrile in various solvents. The reusability of g-C_3N_4 catalyst in Knoevenagel condensation was also studied, which showed that g-C_3N_4 was stable in liquid-phase reactions, whose activity dropped from 74.2% to 63.8% after three regeneration processes.

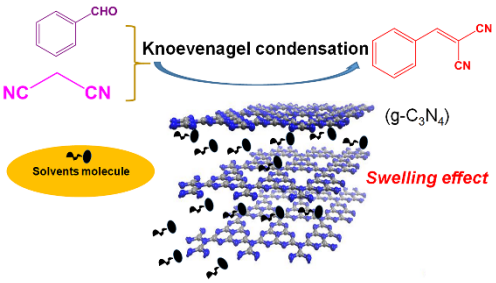

Key Words: g-C_3N_4; Base catalysis; Knoevenagel condensation; Swelling effect

碱催化剂 g-C_3N_4 在液相反应中溶胀特性的研究

吴结群，华伟明，乐英红*，高滋

复旦大学化学系，上海市分子催化和功能材料重点实验室，上海 200438

摘要：通过三聚氰胺、双腈胺、硫脲或尿素的高温热解制备了四种比表面不同的石墨型碳化氮材料(g-C_3N_4)，利用X射线衍射(XRD)、扫描电子显微镜(SEM)、傅里叶变换红外光谱(FTIR)、X射线光电子能谱(XPS)、热重分析(TGA)和N_2吸附方法对所得材料进行结构与表面性质的表征，用CO_2程序升温脱附(CO_2-TPD)和酸碱滴定方法测试了其碱性。考察了这些材料对于

Received: April 17, 2019; Revised: May 5, 2019; Accepted: May 22, 2019; Published online: May 24, 2019.

*Corresponding author. Email: yhyue@fudan.edu.cn; Tel.: +86-21-31249120; Fax: +86-21-65641740.

The project was supported by the National Natural Science Foundation of China (91645201, 21273043), the National Key R&D Program of China (2017YFB0602204), and the Science & Technology Commission of Shanghai Municipality, China (13DZ2275200).

国家自然科学基金(91645201, 21273043), 国家重点研发计划(2017YFB0602204), 上海市科委(13DZ2275200)资助项目

不同溶剂中苯甲醛与丙二腈Knoevenagel缩合反应的催化活性。g-C_3N_4在弱极性溶剂甲苯中的催化活性很低，且活性大小与其比表面和表面碱性密切相关，而在极性溶剂乙醇中四种g-C_3N_4的催化活性则相差不大，且都远高于甲苯中的活性。上述结果无法用常规的碱性表征数据来解释。进一步的实验证明在极性溶剂中g-C_3N_4会发生溶胀，使得表面暴露更多的碱性位，因而催化活性大大提高。不同溶剂中的反应结果表明g-C_3N_4的溶胀效应随反应溶剂的极性增加而增强。重复利用实验表明g-C_3N_4在液相反应中具有良好的稳定性，其对于苯甲醛的转化率在重复利用三次后由74.2%下降至63.8%。

关键词：g-C_3N_4；碱催化；Knoevenagel 缩合；溶胀效应
中图分类号：O643

1 Introduction

Alkali-catalyzed chemical transformations are important industrial processes for fine chemical synthesis [1,2]. Traditional inorganic materials, such as methoxides and hydroxides, are often used as catalysts in many organic reactions, leading to a series of problems such as corrosion toward apparatus, environmental pollutions by metal salt byproducts and difficulty in separation of reactants and products [3,4]. Replacing those unreusable and pollution-causing liquid base catalysts by environmentally benign solid ones has become the dominant trend in the future [5,6]. Thus, the development of more sustainable, efficient and economical heterogeneous base catalysts has come to notice. A lot of solid base catalysts have been studied in the last few decades, such as hydrotalcites [7], apatites [8], metal oxides [9], metal-organic materials [10] and alkali doped zeolites [11]. However, sometimes the results are not satisfying due to the low stability or partial dissolution of the catalysts.

Graphitic carbon nitride (g-C_3N_4) is a kind of polymeric material comprised of s-triazine or s-heptazine units, which is the most stable allotrope of carbon nitrides under ambient conditions. g-C_3N_4 is noteworthy since its excellent surface properties make it applicable in many fields. It can absorb the visible light around 460 nm, which has aroused a great concern as a promising photocatalyst [12–16]. Meanwhile its 2.7 eV energy gap makes it a sort of good semiconductor, being used in the field of electrocatalysis [17,18] and energy storage [19,20]. g-C_3N_4 can also work as a multifunctional catalyst in traditional organic reaction because it has strong nucleophilic abilities, basic surface functionalities and H-bonding motifs due to its unique chemical composition and π-conjugated electronic structure [21,22]. However, much attention of g-C_3N_4 study has been paid to photocatalytic reactions. Detail study on its role as an organocatalyst is still lacking besides its application in Knoevenagel condensations and transesterification reactions [23–25].

In the present work, g-C_3N_4 with different surface areas were synthesized by pyrolysis using various precursors including melamine, dicyandiamide, thiourea and urea. The textural and basic properties were characterized by XRD, SEM, FTIR, XPS, TGA, N_2 adsorption, CO_2-TPD and acid-base titration. The catalytic activities for the liquid-phase Knoevenagel condensation over these catalysts were investigated in various solvents. The swelling effect on the catalytic behavior of the catalysts was investigated and discussed.

2 Experimental

2.1 Materials

Benzaldehyde (> 99.0%), malononitrile (99%), toluene (99.5%), ethanol (≥ 99.5%), dimethyl formamide (> 99.9%), cyclohexane (≥ 99%), furfural (99%), melamine (99%), dicyandiamide (99%), thiourea (99%), and urea (99%) were purchased from Aladdin. All chemical reagents were used as received without further purification.

2.2 Catalyst preparation

Graphitic carbon nitrides were synthesized by bulk condensation pyrolysis of nitrogen-rich precursors. Typically, 10 g melamine, dicyandiamide, thiourea or urea was placed into a covered ceramic crucible and heated at a rate of 2 °C·min^{-1} up to 550 °C, and then maintained at this temperature for 2 h. The resulting product was cooled to room temperature and ground into power. The g-C_3N_4 obtained using melamine, dicyandiamide, thiourea and urea were denoted as MA, DA, TU and UR, respectively.

2.3 Catalyst characterization

XRD patterns were recorded on a D2 PHASER X-ray diffractometer (Bruker, Germany) using nickel-filtered Cu-K_α (λ = 0.15418 nm) at 40 kV and 30 mA in the range of 10°–80°. Infrared spectra (FTIR) of the samples were recorded on a Nicolet iS10 spectrometer (ThermoFisher, USA). SEM measurements were conducted on a Zeiss Ultra-55 electron microscope (Germany) with acceleration voltage of 20.0 kV. XPS measurements were carried out on a Perkin-Elmer PHI 5000C spectrometer (Perkin-Elmer, USA) with Mg K_α radiation ($h\nu$ = 1253.6 eV) as the excitation source. All binding energy values were referenced to the C_{1s} peak at 284.6 eV. The BET surface area and pore volume of the catalysts were analyzed by N_2 adsorption at −196 °C using a Micromeritics ASAP 2000 instrument (Micromeritics, USA). TGA was conducted on a thermal analyzer SETSYS-1750 (SETARAM, France) under air atmosphere with a heating rate of 10 °C·min^{-1}. The measurements were performed in the temperature range of 20–900 °C. The elemental analysis was performed using a Vario EL Elemental Analyzer CHNS-628 (Analysemsysteme GmbH, Germany).

2.4 Basicity measurement

The surface basicity of g-C_3N_4 was evaluated by CO_2-TPD on a Micromeritics AutoChem II instrument (Micromeritics, USA). 150 mg sample (40–60 mesh) was pretreated in He flow at 500 °C for 1 h to remove any adsorbed impurities, then cooled down to 80 °C. The flow was switched to 5% CO_2/He (30 mL·min^{-1}) and kept for 2 h, followed by purging with He (30 mL·min^{-1}) for 1.5 h. The temperature was then raised from 80 °C to 550 °C at a ramping rate of 10 °C·min^{-1}. The CO_2 desorbed was detected by an on-line gas chromatograph (GC) equipped with a thermal conductivity detector (TCD).

The amount of surface base sites was also measured by neutralization titration method. 20 mg of each sample was added to 10 mL aqueous hydrochloric acid solution (0.05 mol·L^{-1}). The mixture was stirred for 30 min with magnetic stirring under N_2 atmosphere. The sample was then removed from the mixture by filtration, and the left solution was immediately titrated with a standard solution of 0.05 mol·L^{-1} sodium hydroxide using phenolphthalein as an indicator.

2.5 Catalytic activity tests

Knoevenagel condensation of benzaldehyde with malononitrile was performed in a 25 mL round-bottom flask equipped with a reflux condenser under magnetic stirring. Typically, 50 mg catalyst was added into the mixture of 1 mmol benzaldehyde and 2 mmol malononitrile with 10 mL solvent. The reaction was carried out at 70 °C for 2 h unless specified. The products of reactions were analyzed with a GC9560 gas chromatograph equipped with a SE-30 capillary column (30 m × 0.25 mm × 0.3 μm). Knoevenagel condensation of furfural and malononitrile is carried out using the same reaction conditions except that the reaction time is 1 h.

Catalyst poisoning test was done by adding a certain amount of benzoic acid to the mixture of catalyst and solvent (toluene or ethanol) prior to the addition of reactants. The above mixture was stirred under room temperature for 10 min. After that, benzaldehyde and malononitrile were added and the catalytic test was done as described above.

3 Results and discussion

3.1 Structural characterization

Fig. 1 exhibited XRD patterns of g-C_3N_4 prepared using melamine, dicyandiamide, thiourea and urea as precursors. Peaks at 2θ of 13.2° and 27.7° are observed for all the samples. The high intensity diffraction peak at 27.7° corresponds to the typical feature (002) interlayer stacking reflection of conjugated aromatic systems. The interlayer distance of aromatic units is 0.33 nm, very close to that of the crystalline g-C_3N_4 (d = 0.34 nm) [26]. The weak peak at 13.2° corresponds to (100) and was interpreted as the in-plane structural repeating motif, probably because of the hole-to-hole distance of the consecutive tri-s-triazine pores [27]. All the XRD patterns of the prepared g-C_3N_4 samples are similar to that of typical crystalline g-C_3N_4, suggesting that the structures of g-C_3N_4 samples are similar regardless of the precursors used. However, the XRD pattern of UR (synthesized from urea) shows a lower and wider peak, indicating its smaller particle size. The generation of O_2 and CO_2 gases in the urea polymerization process was thought to inhibit the condensation graphitic stacking of the C_3N_4 network, resulting in a lower polymerization degree, a smaller particle size and an enlarged surface area [19].

FT-IR is quite useful in characterizing surface functional groups of materials and the FT-IR spectra of our g-C_3N_4 samples are shown in Fig. 2. All of the characteristic vibration modes of typical g-C_3N_4 are clearly seen in the spectra. The strong absorption band located at 1250–1700 cm^{-1} belongs to the typical skeletal stretching vibrations and bending vibrations of the s-triazine or tri-s-trizaine while the sharp peak located at 808 cm^{-1} is ascribed to the breathing modes of the triazine units [28]. The broad band in the range of 3100–3300 cm^{-1} is ascribed to the stretching vibration modes of residual N—H components or the O—H bands, accompanied with uncondensed amino groups and absorbed H_2O molecules, respectively [19]. The weak adsorption observed at 2350 cm^{-1} is due to CO_2 molecules adsorbed on g-C_3N_4 surface [29].

The elemental analysis was carried out to determine the composition of the prepared g-C_3N_4. The results summarized in Table 1 show that all samples contain a minor portion of hydrogen element besides carbon and nitrogen, which is related to the presence of amino (primary and secondary) groups in the peripheral parts of g-C_3N_4 layers [30]. No big difference about the hydrogen contents was found among all the samples. The carbon to nitrogen ratios of the samples are almost the same of 0.63,

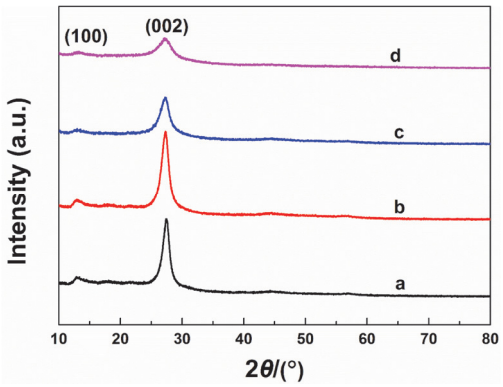

Fig. 1 XRD patterns of (a) MA, (b) DA, (c) TU, and (d) UR.

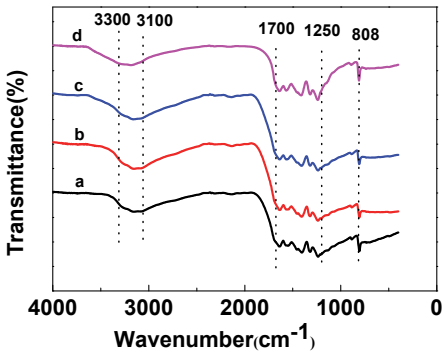

Fig. 2 FT-IR spectra of (a) MA, (b) DA, (c) TU, and (d) UR.

Table 1 Elemental analysis and composition (*w*, mass fraction) of carbon nitrides (g-$C_xN_yH_z$).

Sample	w_C/%	w_N/%	w_H/%	*x*	*y*	*z*	C/N ratio
MA	34.4	63.6	2.0	5.7	9.1	4.0	0.63
DA	34.4	63.4	2.2	5.7	9.1	4.4	0.63
TU	34.0	62.9	2.2	5.7	9.0	4.4	0.63
UR	34.1	62.5	2.2	5.7	8.9	4.4	0.64

lower than the ratio of 0.75 for the ideal C_3N_4. This finding suggests that all the products are nitrogen-rich materials in which the most likely form of nitrogen is the amino group caused by the incomplete condensation of the heptazine units. The SEM images of the prepared g-C_3N_4 samples are illustrated in Fig. 3. The precursor also has a marked impact on the morphology of the ultimate g-C_3N_4. Unlike MA, DA and TU which are made up of irregular layered structures, UR is mostly composed of smaller particles and sheets, and its interior pore structure can be observed clearly.

The N_2 adsorption-desorption isotherms of the samples were recorded and shown in Fig. 4. All samples display the Type IV isotherm, indicating their similar stacked-layer structure. The hysteresis loop at high relative pressure is more evident and larger for UR, indicating the existence of a larger amount of mesopores and macropores within the structure. Table 2 summarizes the textural properties of the prepared g-C_3N_4 samples. It can be seen that the surface area is quite different by using different precursors. UR has the highest surface area, which is in accord with the XRD and SEM results.

The surface composition and chemical state of the elements in the synthesized samples were determined by XPS. The surface of the four samples contain C, N and O elements and their spectra are almost the same, indicating that the surface compositions and chemical states of MA, DA, TU and UR remain the same regardless of their precursor (shown in Fig. S1, Supporting Information). The C_{1s} spectra can be deconvoluted into two peaks with binding energy of 284.6 eV (C1) and 287.5 eV (C2), as shown in Fig. S1. The former peak corresponds to －C＝ of aromatic ring while the latter belongs to N＝C－N of triazine ring [31]. The N_{1s} spectra are composed of three peaks centered at 397.9 eV (N1), 398.8 eV (N2) and 400.3 eV (N3).

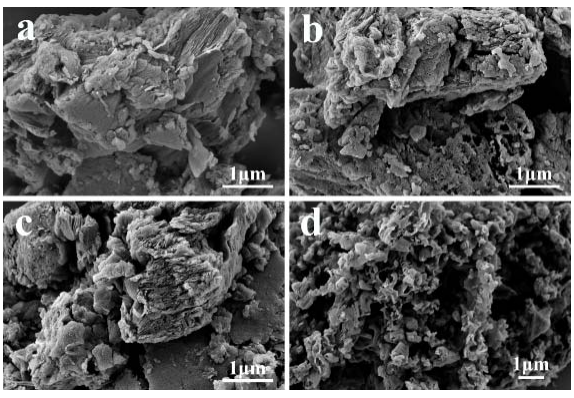

Fig. 3 SEM images of (a) MA, (b) DA, (c) TU, and (d) UR.

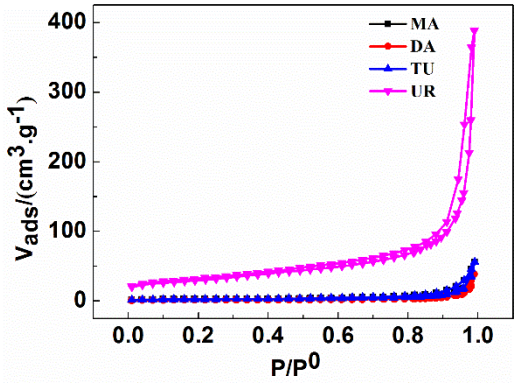

Fig. 4 The N_2 adsorption-desorption isotherms of the samples.

Table 2 Textural and basic properties of carbon nitrides.

Sample	Textural properties		Amount of base sites	
	Surface areas/ ($m^2 \cdot g^{-1}$)	Pore volume/ ($cm^3 \cdot g^{-1}$)	CO_2-TPD/ (mmol·g^{-1})	Titration/ (mmol·g^{-1})
MA	7.9	0.087	0.08	0.75
DA	5.2	0.060	0.09	0.81
TU	23.7	0.175	0.21	1.31
UR	103	0.601	0.24	1.36

The N1 peak assigning to nitrogen sp^2-bonded to carbon (C－N＝C) indicates the existence of triazine rings, while the N2 and N3 peaks are related to the existence of the C－N－H and N－$(C)_3$ bonding, respectively [32]. The O_{1s} spectra are probably due to the adsorption of H_2O or CO_2 molecules on the surface [33], which consists with the FT-IR measurements.

The thermographic (TG) analysis was conducted under air atmosphere. As shown in Fig. 5, a slight loss of weight resulting from the desorption of H_2O or CO_2 is observed at the temperature of 20–200 °C [34]. All the g-C_3N_4 samples are quite stable until the temperature reaches 550 °C, and no residues of the samples are left above 650 °C. UR is slightly less stable than the other three g-C_3N_4, probably due to its lower polymerization degree.

3.2 Basicity of the catalysts

The surface basicities of the g-C_3N_4 samples were measured by CO_2-TPD, and the results are given in Table 2. There is only one broad peak on the TPD profiles of the four samples (Fig. S2),

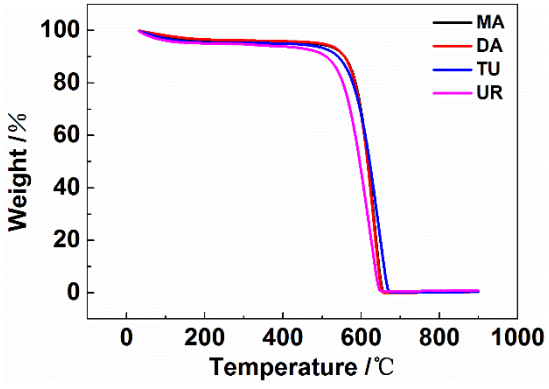

Fig. 5 TG thermograms of the samples.

and the peak temperatures are all in the range of 124–136 °C, showing that the base sites are of weak strength. The number of base sites on g-C_3N_4 samples depends greatly on the precursor used, which decreases in the order of UR > TU > DA ≈ MA, following exactly the same sequence of their surface area. This indicates that the larger the surface area, the more exposed base sites.

The amount of surface base sites was also evaluated by titration in aqueous solution. The results obtained are shown in Table 2. The amount of base sites also changes in proportion to the surface area. However, it is interesting that the data obtained from titration are much larger than those from CO_2-TPD, showing that more base sites are accessible in solution than in gas phase. It should be possible, similar result was reported that only 6% Brönsted acid sites of MCM-22 were detected by ^{31}P MAS NMR study when using large base probe adsorption [35].

3.3 Catalytic activity

Knoevenagel condensation reaction between benzaldehyde with malononitrile was selected as the base-catalyzed probe reaction to evaluate the catalytic activity of g-C_3N_4 synthesized from different precursors. The reaction was carried out both in toluene and ethanol, and the results are summarized in Table 3. All the g-C_3N_4 catalysts are moderately active in toluene, but their activities differ a lot. The conversion of benzaldehyde decreases in the order of UR > TU > DA ≈ MA, in accord with the decrease of surface area and surface base sites. While in ethanol, the situation becomes totally different. The catalysts are much more active, and no obvious difference in activity can be observed among the four g-C_3N_4 catalysts. After reacting for 0.5 and 2 h, the conversions of benzaldehyde for all the catalysts reach above 61% and 92%, respectively.

It was reported that the reaction rate of Knoevenagel condensation was affected by the polarity of the solvent, since the reaction involved charged species [36]. A higher yield of the condensed product from benzaldehyde and ethyl cyanoacetate was obtained in more polar solvents such as EtOH and DMF than in nonpolar solvent such as toluene, probably due to their different electrostatic field in the reaction media [36]. However, the reported difference caused by solvent effect over heterogeneous catalysts such as functionalized polyacrylonitrile fiber [37] or amines embedded MOFs [38] was not so evident as ours. Meanwhile, the solvent effect mentioned cannot explain the similar activity of our catalysts with different surface area and basicity in ethanol solution. The above results show that something more important than single solvent effect must be involved under our present reaction conditions.

Table 3 Activity of carbon nitrides for Knoevenagel condensation.

Catalysts	Conversion (%)	
	in ethanol [a]	in toluene
MA	95.4 (61.5)	9.7
DA	94.3 (64.6)	9.0
TU	92.2 (66.9)	15.2
UR	96.8 (74.2)	23.7

[a] The values inside the brackets are obtained at 0.5 h.

The basicity measurement results listed in Table 2 show that more base sites can be detected in aqueous solution than that in gas-phase, indicating that the amount of accessible base sites are quite different under different conditions. The above results indicate that different amounts of accessible base sites may account for the different activity in toluene and in ethanol. To prove this hypothesis, the amount of active sites of UR during reaction in toluene and in ethanol was estimated by the catalyst poisoning method. As we can see from Fig. 6, the conversion in toluene dropped dramatically with the adding of benzoic acid. When the adding amount was increased to 40.9 mmol·g^{-1}, the catalyst totally lost its activity. The conversion in ethanol also decreased with the amount of benzoic acid adsorption. However, the dropping rate was much slower as compared with that in toluene. The poisoned catalyst was still active until the adding amount reached over 143.3 mmol·g^{-1}. The different results for the two solvents indicated that different amounts of accessible base sites participated in the liquid-phase reaction using the same catalyst.

For sulfonated carbon catalysts, swelling in liquid solutions was found to be essential for better catalytic performance [39]. All the above experimental results inspired us that g-C_3N_4 catalysts with layered structure might swell as well in polar solvents. Therefore, XRD experiment of the UR sample after treated with ethanol was carried out. As demonstrated in Fig. 7a, an additional peak at 21.7° appeared, showing that the intercalation of polar solvent molecules between the layers in the structure occurred in the swollen sample and part of the interlayer distance was increased. The peak disappeared after the UR sample was dried by heating (Fig. 7b). The swelling caused a significant increase in the amount of accessible basic sites on the catalyst, so that the above results of uncommonly high surface acidity and catalytic activity for UR in polar ethanol solution were obtained, which can not be explained by the results obtained from the conventional basicity measurements.

To further confirm the swelling effect of solvents, several other commonly used solvents in organic reactions such as DMF and cyclohexane were employed besides ethanol and toluene for

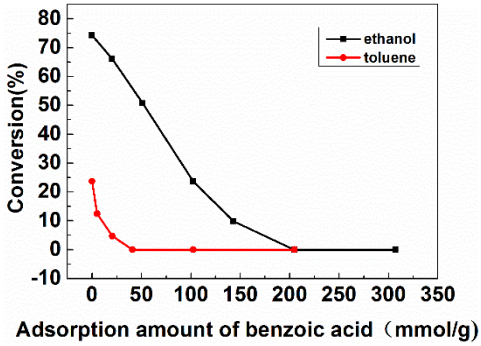

Fig. 6 Relevance of amount of benzoic acid and the conversion of benzaldehyde.

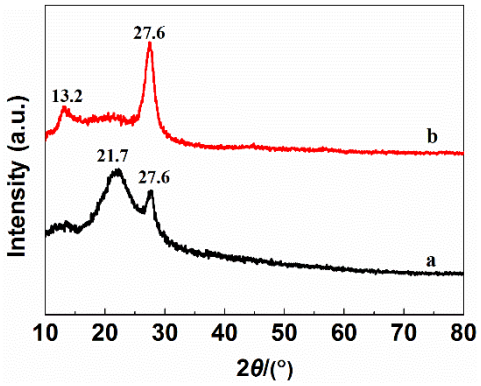

Fig. 7 XRD patterns of (a) UR with ethanol, and (b) UR without ethanol.

short-term reaction tests. As shown in Table 4, the benzaldehyde conversion decreases in the order of DMF > ethanol > toluene > cyclohexane, which is exactly the same as the order of the drop of their polarity. Knoevenagel condensation of furfural and malononitrile was also carried out over UR in these solvents. Similar sequence can be obtained (see Table 4), which indicates that the swelling effect of different solvents depends considerably on its polarity.

The reusability of UR catalyst in Knoevenagel condensation of benzaldehyde and malononitrile was also studied in ethanol. After reaction, the catalyst was filtered out from the solution, dried by heating and then reused. The results were illustrated in Fig. 8. The activity of the catalyst decreases very slowly in succession, whose conversion drops from 74.2% to 63.8% after three regeneration process, showing that g-C_3N_4 is quite stable in liquid-phase reactions.

Table 4 Effect of solvents on Knoevenagel condensation.

Solvent	Polarity	Boiling point/°C	Conversion/%	
			benzaldehyde	furfur
dimethyl formamide	6.4	153	77.5 [a]	68.5
ethanol	4.3	79	74.2 [a]	62.7
toluene	2.4	111	23.7	14.7
cyclohexane	0.1	81	6.7	5.4

[a] The values are obtained at 0.5 h.

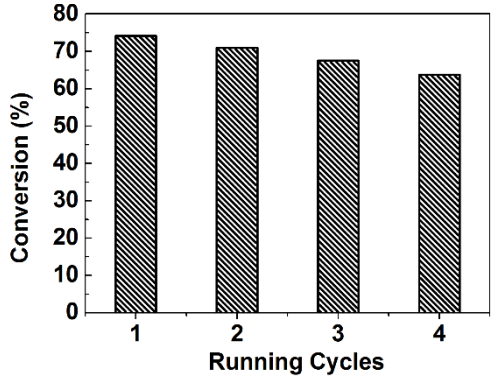

Fig. 8 Activities of reused UR catalysts in ethanol.

4 Conclusions

Graphitic carbon nitrides are solid base catalysts of weak strength. They are active for the liquid-phase Knoevenagel condensation of benzaldehyde and malononitrile. Basicity measurements and catalytic activity tests in this work show that the effect of the solvents used in the liquid-phase reaction is critical. Polar solvent gives much higher conversion than non-polar solvent, because catalyst swelling in polar solvent increases the amount of exposed base sites on the surface of g-C_3N_4 catalysts significantly. The results of a comparison between the swelling effects of different solvents show that they are mainly affected by the polarity of the solvents. The higher the polarity of the solvent is, the better the swelling effect behaves.

Acknowledgement: Zi Gao, Yinghong Yue and Weiming Hua have been members of the Key Research Projects, “Molecular Engineering of Creation of New Materials”, of National Education Department and National Scientific Research Department led by Prof. Youqi Tang. We are very grateful for his care, helps and precious advices. Our research group learned a lot while working on the projects. On his 100th birthday, we want to express our heartfelt thanks to our most respectful teacher noted for his advanced scientific ideas and meticulous scholarship and wish him good health and a long life.

Supporting Information: available free of charge *via* the internet at http://www.whxb.pku.edu.cn.

References

(1) Tanabe, K.; Holderich, W. F. *Appl. Catal. A* **1999,** *181*, 399. doi: 10.1016/S0926-860X(98)00397-4

(2) Davis, R. J. *J. Catal.* **2003,** *216*, 396. doi: 10.1016/S0021-9517(02)00034-9

(3) Blaser, H. U. *Catal. Today* **2000,** *60*, 161. doi: 10. 1016/S0920-5861(00)00332-1

(4) Kelly, G. J.; King, F.; Kett, M. *Green Chem.* **2002,** *4*, 392. doi: 10.1039/B201982P

(5) Wight, A. P.; Davis, M. E. *Chem. Rev.* **2002,** *102*, 3589. doi: 10.1021/cr010334m

(6) Diaz, U.; Garcia, T.; Velty, A.; Corma, A. *J. Mater. Chem.* **2009,** *19*, 5970. doi: 10.1039/B906821J

(7) Climent, M. J.; Corma, A.; Iborra, S.; Velty, A. *J. Catal.* **2004,** *221*, 474. doi: 10.1016/j.jcat.2003.09.012

(8) Sebti, S.; Solhy, A.; Tahir, R.; Smahi, A. *Appl. Catal. A-Gen.* **2002,** *235*, 273. doi: 10.1016/S0926-860X(02)00273-9

(9) Liu, Z.; Cortes-Concepcion, J. A.; Mustian, M.; Amiridis, M. D. *Appl. Catal. A-Gen.* **2006,** *302*, 232. doi: 10.1016/j.apcata.2006.01.007

(10) Wang, X. G.; Tseng, Y. H.; Chan, J. C. C.; Cheng, S. F. *J. Catal.* **2005,** *233*, 266. doi: 10.1016/j.jcat.2005.04.007

(11) Goa, Y.; Wu, P.; Tatsumi, T. *J. Catal.* **2004,** *224*, 107. doi: 10.1016/j.jcat.2004.01.021

(12) Wang, X.; Maeda, K.; Thomas, A.; Takanabe, K.; Xin, G.; Carlsson, J. M.; Domen, K.; Antonietti, M. *Nat. Mater.* **2009,** *8*, 76. doi: 10.1038/nmat2317

(13) Wang, Y.; Wang, X. C.; Antonietti, M. *Angew. Chem. Int. Ed.* **2012,** *51*, 68. doi: 10.1002/anie.201101182

(14) Praus, P.; Svoboda, L.; Ritz, M.; Troppova, I.; Sihor, M.; Koci, K. *Mater. Chem. Phys.* **2017,** *193*, 438. doi: 10.1016/j.matchemphys.2017.03.008

(15) Chi, S. H.; Ji, C. N.; Sun, S. W.; Jiang, H.; Qu, R. J.; Sun, C. M. *Ind. Eng. Chem. Res.* **2016,** *55*, 12060. doi: 10.1021/acs.iecr.6b02178

(16) Zhang, G. G.; Zhang, J. S.; Zhang, M. W.; Wang, X. C. *J. Mater. Chem.* **2012,** *22*, 8083. doi: 10.1039/C2JM00097K

(17) Zhai, H. S.; Cao, L.; Xia, X. H. *Chin. Chem. Lett.* **2013,** *24*, 103. doi: 10.1016/j.cclet.2013.01.030

(18) Yew, Y. T.; Lim, C.S.; Eng, A. Y. S.; Oh, J.; Park, S.; Pumera, M. *ChemPhysChem* **2016,** *17*, 481. doi: 10.1002/cphc.201501009

(19) Datta, K. K. R.; Reddy, B. V. S.; Ariga, K.; Vinu, A. *Angew. Chem. Int. Ed.* **2010,** *49*, 5961. doi: 10.1002/anie.201001699

(20) Wang, Y.; Yao, J.; Li, H.; Su, D.; Antonietti, M. *J. Am. Chem. Soc.* **2011,** *133*, 2362. doi: 10.1021/ja109856y

(21) Goettmann, F.; Fischer, A.; Antonietti, M.; Thomas, A. *Angew. Chem. Int. Ed.* **2006,** *45*, 4467. doi: 10.1002/anie.200600412

(22) Ansari, M. B.; Min, B. H.; Mo, Y. H.; Park, S. E. *Green Chem.* **2011,** *13*, 1416. doi: 10.1039/C0GC00951B

(23) Zhang, L.; Wang, H.; Shen, W. Z.; Qin, Z. F.; Wang, J. G.; Fan, W. B. *J. Catal.* **2016,** *344*, 293. doi: 10.1016/j.jact.2016.09.023

(24) Su, F. Z.; Antoniettia, M.; Wang, X. C. *Catal. Sci. Technol.* **2012,** *2*, 1005. doi: 10.1039/C2CY00012A

(25) Xu, J.; Wang, Y.; Shang, J. K.; Jiang, Q.; Li, Y. X. *Catal. Sci. Technol.* **2016,** *6*, 4192. doi:10.1039/C5CY01747E

(26) Yan, S. C.; Li, Z. S.; Zou, Z. G. *Langmuir* **2009,** *25*, 10397. doi: 10.1021/la900923z

(27) Kawaguchi, M.; Nozaki, K. *Chem. Mater.* **1995,** *7*, 257. doi:10.1021/cm00050a005

(28) Thomas, A.; Fischer, A.; Goettmann, F.; Antonietti, M.; Muller, J. O.; Schlogl, R.; Carlsson, J. M. *J. Mater. Chem.* **2008,** *18*, 4893. doi: 10.1039/B800274F

(29) Kauffman, K. L.; Culp, J. T.; Goodman, A.; Matranga, C. *J. Phys. Chem. C.* **2011,** *115*, 1857. doi: 10.1021/jp102273w

(30) Komatsu, T.; Nakamura, T. *J. Mater. Chem.* **2001,***11*, 474. doi: 10.1039/B005982J

(31) Wang, X. C.; Chen, X. F.; Thomas, A.; Fu, X. Z.; Antonietti, M. *Adv. Mater.* **2009,** *21*, 1609. doi: 10.1002/adma.200802627

(32) Pinero, E. R.; Amoros, D. C.; Solano, A. L.; Find, J.; Wild, U.; Schlogl, R. *Carbon* **2002,** *40*, 597. doi: 10.1016/S0008-6223(01)00155-5

(33) Cui, Y. J.; Zhang, J. S.; Zhang, G. G.; Huang, J. H.; Liu, P.; Antonietti, M.; Wang, X. C. *J. Mater. Chem.* **2011,** *21*, 13032. doi: 10.1039/C1JM11961C

(34) Yan, H. J.; Chen, Y.; Xu, S. M. *Int. J. Hydrog. Energy* **2012,** *37*, 125. doi: 10.1016/j.ijhydene.2011.09.072

(35) Wang, Y.; Zhuang, J. Q.; Yang, G.; Zhou, D. H.; Ma, D.; Han, X. W.; Bao, X. H. *J. Phys. Chem. B* **2004,** *108*, 1386. doi: 10.1021/jp034989y

(36) Rodriguez, I.; Sastre, G.; Corma, A.; Iborra, S. *J. Catal.* **1999,** *183*, 14. doi: 10.1006/jcat.1998.2380

(37) Li, G. W.; Xiao, J.; Zhang, W. Q. *Green Chem.* **2011,** *13*, 1828. doi: 10.1039/C0GC00877J

(38) Burgoyne, A. R.; Meijboom, R. *Catal. Lett.* **2013,** *143*, 563. doi: 10.1007/s10562-013-0995-5

(39) Mo, X. H.; López, D. E.; Suwannakarn, K.; Liu, Y. J.; Lotero, E.; Goodwin, J. G., Jr.; Lu, C. Q. *J. Catal.* **2008,** *254*, 332. doi: 10.1016/j.jcat.2008.01.011